



Published in final edited form as:

*J Biol Chem.* 2003 July 25; 278(30): 28237–28245. doi:10.1074/jbc.M302651200.

## RNA-structural Mimicry in *Escherichia coli* Ribosomal Protein L4-dependent Regulation of the *S10* Operon\*

Ulrich Stelzl<sup>‡,§,¶</sup>, Janice M. Zengel<sup>||</sup>, Marina Tovbina<sup>‡</sup>, Marquis Walker<sup>||</sup>, Knud H. Nierhaus<sup>§</sup>, Lasse Lindahl<sup>||</sup>, and Dinshaw J. Patel<sup>‡</sup>

<sup>‡</sup>Memorial Sloan Kettering Cancer Center, Cellular Biochemistry and Biophysics Program, New York, New York 10021

<sup>§</sup>Max-Planck-Institut für Molekulare Genetik, AG Ribosomen, Ihnestrasse 73, D-14195 Berlin, Germany

<sup>||</sup>Department of Biological Sciences, University of Maryland, Baltimore County, Baltimore, Maryland 21250

### Abstract

Ribosomal protein L4 regulates the 11-gene *S10* operon in *Escherichia coli* by acting, in concert with transcription factor NusA, to cause premature transcription termination at a Rho-independent termination site in the leader sequence. This process presumably involves L4 interaction with the leader mRNA. Here, we report direct, specific, and independent binding of ribosomal protein L4 to the *S10* mRNA leader *in vitro*. Most of the binding energy is contributed by a small hairpin structure within the leader region, but a 64-nucleotide sequence is required for the *bona fide* interaction. Binding to the *S10* leader mRNA is competed by the 23 S rRNA L4 binding site. Although the secondary structures of the mRNA and rRNA binding sites appear different, phosphorothioate footprinting of the L4-RNA complexes reveals close structural similarity in three dimensions. Mutational analysis of the mRNA binding site is compatible with the structural model. *In vitro* binding of L4 induces structural changes of the *S10* leader RNA, providing a first clue for how protein L4 may provoke transcription termination.

Ribosomal proteins are encoded on the bacterial chromosomes in multigene operons that facilitate stoichiometric production of the more than 50 ribosomal proteins (r-proteins).<sup>1</sup> Expression of most of these operons is translationally regulated by a single regulatory r-protein encoded by a given polycistronic mRNA. This operon-specific autogenous control mechanism is elicited when repressor r-proteins are not consumed during the assembly of ribosomal subunits. In the absence of sufficient ribosomal RNA targets, the resulting excess of “free” repressor proteins bind to their own mRNAs and block translation of the polycistronic mRNA (reviewed in Refs. 1 and 2).

\*This work was supported by the National Institutes of Health Grant CA46778 (to D. J. P.) and NIGMS, National Institutes of General Medical Science Grant 54876 (to J. M. Z. and L. L.).

<sup>¶</sup>To whom correspondence should be addressed. Present address: Max-Delbrück-Centrum für Molekulare Medizin (MDC), Robert-Rössle-Straße 10, D-13092 Berlin-Buch, Germany. Tel.: 49-30-9406-2354; Fax: 49-30-9406-2552; u.stelzl@mdc-berlin.de.

<sup>1</sup>The abbreviations used are: r-protein, ribosomal protein; nt, nucleotide(s); BSA, bovine serum albumin; L4EC, L4 from *E. coli*; *E. coli* numbering is used if not indicated otherwise.

R-protein L4 from *Escherichia coli* specifically regulates the *S10* operon, which codes for 11 r-proteins including L4 itself (3, 4). L4 is unique among the regulatory ribosomal proteins because it regulates not only translation but also transcription of the *S10* operon mRNA. The latter form of regulation is accomplished by L4 stimulation of transcription termination at a terminator (attenuator) structure in the mRNA upstream of the initiation codon of the first gene of the operon (5). Determinants necessary for L4-mediated autogenous control are contained within a 172-nucleotide 5'-untranslated region of the *S10* operon mRNA. This region folds into six stem-loop structures termed helices HA, HB, HC, HD, HE, and HG (Fig. 1A) (6, 7).

The mRNA sequences necessary for L4-mediated transcription and translation control overlap, but are not identical (8, 9). Helix HE and the unstructured sequence immediately downstream of this hairpin are necessary for translational control, whereas helices HD and HE are required for transcriptional control (8, 10, 11). L4-stimulated transcription termination occurs within the U cluster (nt 139–149) (9) in helix HE, which resembles a Rho-independent terminator. *In vitro* transcription experiments (10, 12) suggest that the transcription attenuation process involves three ordered steps: (i) spontaneous pausing of the RNA polymerase at the attenuation site, (ii) NusA-mediated stabilization of the pause, and (iii) additional stabilization of the pause involving protein L4 that leads to transcription termination.

Binding of a regulatory r-protein to specific targets in both rRNA and mRNA is fundamental to the autogenous control model (13). The minimal rRNA target of L4, identified by serial selection of random *E. coli* rRNA fragments binding to L4 (14), is a four-helix junction composed of nucleotides 295–343 in Domain I of the 23 S rRNA. Binding of protein L4 to this RNA sequence generates a characteristic iodine cleavage pattern in the U321-loop of 23 S rRNA (15). Interestingly, the same region of 23 S rRNA competes with the paused transcription complex for L4, eliminating the ability of the protein to stimulate transcription termination (16). These results show that binding of 23 S rRNA to L4 inactivates the regulatory capacity of the protein and suggest that the 23 S rRNA and mRNA binding sites for L4 might share certain critical features. However, mutations in protein L4 can distinguish its ability to regulate the expression of the *S10* operon from its ability to be incorporated into the ribosome (17).

Here we demonstrate direct binding of r-protein L4 to the *S10* mRNA leader. Furthermore, we analyze the requirements in the RNA binding site for L4 binding. Footprinting results indicate structural changes of the leader RNA upon binding, and reveal structural similarities between the rRNA and mRNA L4 binding sites. A structure model for the L4-mRNA interaction is proposed.

## EXPERIMENTAL PROCEDURES

### Protein Expression and Purification

Protein L4 from *E. coli* (L4EC) was purified from 50 S subunits as described (18). The clone of the full-length *Thermus aquaticus* L4 protein was a kind gift from Dr. Alexander Mankin (University of Illinois, Chicago, IL). Protein L4THD7 is a variant of *T. aquaticus*

L4 with a deletion in which 46 amino acids (Thr<sup>46</sup> to Lys<sup>91</sup>, corresponding to Thr<sup>43</sup> to Arg<sup>88</sup> in *E. coli*, Fig. 1B) were replaced with a single glycine. The gene was cloned into pET29b (Novagen), protein L4THD7 was expressed in *E. coli* BL21(DE3) and purified from the soluble cell extract via affinity chromatography on Ni<sup>2+</sup>-agarose (Qiagen). The histidine tag was cleaved off with thrombin and the resulting L4THD7 protein was further purified via ion exchange chromatography where it eluted from a Mono S column (Amersham Biosciences) at 270 mM KCl. The protein was >95% pure and did not exhibit RNase activity.

### In Vivo Regulatory Studies

The regulatory capacity of the *T. aquaticus* L4 proteins was determined as described (7). A C-terminal 6-histidine tag (no thrombin cleavage site) was introduced into both L4TH (wt) and L4THD7 genes, and the genes were placed under control of an arabinose-inducible promoter in a pBAD18 derivative. The plasmids were introduced into *E. coli* K12 strain LL308 containing target plasmid pACYC-*S10'*/*lacZ* or pACYC- HD-*S10'*/*lacZ*. Plasmid pACYC-*S10'*/*lacZ* contains the entire *E. coli* S10 leader and proximal 54 codons of the S10 structural gene, fused in-frame with a *lacZ* gene (lacking the proximal 8 codons), and under control of the isopropyl-1-thio- $\beta$ -D-galac-topyranoside-inducible *trc* promoter. This plasmid contains the regulatory signals necessary for both transcription and translation control of  $\beta$ -galactosidase synthesis by r-protein L4 (19). Plasmid pACYC- HD-*S10'*/*lacZ* is a derivative of pACYC-*S10'*/*lacZ* that has a deletion of the S10 leader hairpin HD eliminating L4-mediated transcription control (11).

### S10 Leader mRNA Constructs

Plasmid pT724 (which encodes the entire S10 operon leader and proximal one and a half structural genes (6)) was used as PCR template to amplify various parts of the S10 leader mRNA. The PCR products were cloned into the *Bam*HI/*Eco*RI site of pSP65 (Promega). The 5'(+ ) primer introduced a T7 promoter, and the 3'(-) primer introduced a restriction site for linearization of the plasmid for run-off T7 RNA polymerase transcription (20). We used constructs with transcription starts at four sites of the leader: (i) at HA with G1 as the first nucleotide, (ii) at HE with the start at GGG-C86, (iii) at HD with the start at GG-A62, and (iv) at HD with the start at GG-A64 (Fig. 1, *green arrows*). The two nucleotide differences in the latter two constructs had no effect on the experimental results reported. The 3' termini of the RNA transcripts were generated by digestion of the templates with restriction enzymes *Ssp*I (after helix HC at U66), *Sna*BI (after HD at C86), *Bsa*I (in the lower HE at C100), *Hpa*I (C125 after the upper HE at C125), *Dra*I (after HE at U147), or *Sma*I (after HG at C197) (Fig. 1A, *red brackets*). We also made a construct encoding a transcript with a hammerhead generating the C125 end.

### Nitrocellulose Filter Binding Assays

Nitrocellulose filtration assays, described in Ref. 20, were done in 300- $\mu$ l reactions containing 20 mM HEPES-KOH (pH 7.5), 4 mM MgCl<sub>2</sub>, 4 mM  $\beta$ -mercaptoethanol, 200–400 mM NH<sub>4</sub>Cl, RNase-free BSA and tRNA bulk (as indicated). Binding data were fitted to single site hyperbolic curves (Fig. 1, *upper panel*). In competition assays, the L4

concentration was  $0.67 \mu\text{M}$  and  $^{32}\text{P}$ -labeled RNA A–G (500–1500 dpm/pmol) was  $0.33 \mu\text{M}$ . Under these conditions about 22 pmol of complex was collected on the nitrocellulose filter. Competitor (*i.e.* non-labeled) RNA was added to labeled RNA A–G before the refolding step. Competition data were fitted with the program Sigma Plot according to Equation 5 of Lin and Riggs (21) solved for the fraction of labeled RNA bound (Fig. 1, *middle* and *lower panel*).

### Gel Shift Assays

A 15- $\mu\text{l}$  sample of an RNA-protein complex containing 75 pmol of [ $^{32}\text{P}$ ]RNA and the indicated amount of protein L4 was prepared by incubating for 15 min at  $37^\circ\text{C}$  (20 mM Hepes-KOH (pH 7.4), 100 mM  $\text{NH}_4\text{Cl}$ , 4 mM  $\text{MgCl}_2$ , 10% glycerol) and then chilling on ice. The sample was loaded onto a buffered (20 mM Hepes-KOH (pH 7.4), 100 mM  $\text{NH}_4\text{Cl}$ , 4 mM  $\text{MgCl}_2$ ) 5% acrylamide/bisacrylamide (29/1) gel ( $0.75 \times 130 \times 170$  mm). The gel was run at 110 V for 2 h at  $4^\circ\text{C}$  and the electrode buffer was recirculated between the electrode chambers with a pump. The gels were dried and exposed on a phosphoimaging plate (Fuji) for quantification.

### Iodine Footprinting

The experiments were done as described previously for the complex of ribosomal RNA with protein L4 (15). Phosphorothioated RNA was produced by including  $S_{\text{P}}\text{-}[\alpha\text{-S}]\text{NTPs}$  (PerkinElmer Life Sciences and Glen Research) in the T7 RNA polymerase transcription assay. The L4 concentration was  $0.67 \mu\text{M}$  and that of  $^{32}\text{P}$ -labeled phosphorothioated RNA was  $0.33 \mu\text{M}$  or vice versa (the yield of complex was identical in both experiments). As seen in some experiments, the mRNA fragments tend to break at C38-A39 and C63-A64 even in the absence of iodine, and at G80-A81 in the presence of L4THD7. However, in general control experiments carried out without addition of iodine did not result in cleavages.

## RESULTS

### Binding of Protein L4EC to the S10 mRNA Leader RNA in Vitro

To analyze L4 interaction with the S10 leader, we modified the strategy previously used to demonstrate L4 binding to its target in Domain I of 23 S rRNA. Ribosomal protein L4EC was incubated with  $^{32}\text{P}$ -labeled S10 leader RNA, or, as a control, its known target in 23 S rRNA, and subjected to nitrocellulose filtration. The results in Fig. 2 (*top panel*) demonstrated that the full-length leader mRNA (A-G, 1–197C) bound r-protein L4 with an apparent  $K_D$  of about 700 nM (in 4 mM  $\text{MgCl}_2$ , 250 mM  $\text{NH}_4\text{Cl}$ ; binding was strongly dependent on the ionic condition). The affinity is in the same range as reported for the S4- $\alpha$  mRNA (22) and the S7-*str* mRNA interaction (23). The interaction of L4 with the full-length S10 leader mRNA was about 4-fold weaker than with its cognate rRNA target in Domain I of 23 S rRNA (GG295–343CC; rRNA-DI, 53 nt) (14). Control RNAs such as G600-C657 from Domain II of 23 S rRNA (rRNA-DII) did not bind, even though this part of the 23 S rRNA contains a site that cross-links to L4 in the intact ribosome (24). Other control RNAs, *e.g.* fragments of ribosomal RNA of various lengths (50 to 170 nt), also failed to bind r-protein L4 (data not shown). Likewise, the sequence comprising the first three helices from the beginning of the S10 leader sequence did not bind (Fig. 2 *top*, A–C,

1–66). This result suggests that the S10 leader contains one or more sites for L4 binding downstream of the HC hairpin.

Because many highly positively charged ribosomal proteins, such as L4, bind with considerable strength to nonspecific RNAs (*e.g.* Refs. 25 and 26), we tested the specificity of L4 binding to the S10 leader by competition experiments (Fig. 2, *middle panel*). As expected, non-radioactive S10 leader RNA (A–G) competes with binding of radioactive leader RNA. In contrast, addition of a 218-nt mRNA molecule that contains the interaction site for r-protein S15 in the translational regulation of the *rpsO* operon (27) did not affect complex formation between the cognate S10 leader mRNA and L4. Thus, the affinity of L4 for the S10 leader mRNA is significantly higher than its affinity for a noncognate r-operon mRNA, indicating that the L4-S10 leader interaction is specific. On the other hand, the rRNA binding site of ribosomal protein L4 (RNA-DI) strongly competes with binding to the S10 leader mRNA (Fig. 2, *middle*). Not assuming allosteric effects, this observation is consistent with the hypothesis that the L4 binding sites on 23 S rRNA Domain I and the S10 leader share significant structural features.

To define the binding site more precisely, we tested various S10 leader mRNA subdomains in the competition experiments (Fig. 2, *bottom panel*). Most intriguingly, the mRNA fragments that do not contain helix HD, such as A–C (66 nt), E (65 nt), and E–G (116 nt), do not inhibit complex formation, whereas the isolated helix HD (D, 27 nt) competes significantly. All other constructs containing HD (*viz.* A–D (86 nt), D–E (88 nt), and D–G (139 nt)) compete to the same extent as the full-length A–G (198 nt). Consistent with data indicating the importance of helix HD in L4-dependent transcription regulation (11, 28), these experiments suggest that helix HD contributes the most to the specificity of L4 binding.

## T. aquaticus Protein L4 Actively Regulates E. coli S10 Operon Expression

Protein L4 from *E. coli* is not well suited for *in vitro* binding experiments, because (i) it has to be purified under denaturing conditions either from ribosomes or from inclusion bodies, (ii) it is relatively unstable, (iii) the solubility even in high salt buffers is very low (<50  $\mu$ M), and (iv) it aggregates even at low concentrations. For example, in gel-shift experiments RNA-L4EC complexes form aggregates that remain for the most part in the gel pocket (not shown).

To circumvent these problems we combined two strategies to develop a better behaved protein. First, because L4 proteins from many other eubacteria regulate the *E. coli* S10 operon (7, 19), we switched to L4 from *T. aquaticus* (L4TH), which is 34% identical and 50% similar to L4 from *E. coli* (Fig. 1B). Proteins from such thermophilic bacterial species have proven to be beneficial for other biochemical and biophysical experiments. Second, we deleted 46 amino acids that, in the ribosome, form an extension protruding into the core from a globular domain located on the surface of the ribosome (29, 30) (*cf.* Figs. 1B and 4C). In free L4 protein (from *Thermotoga maritima*) the corresponding amino acids are not organized into a particular structure (31), and hence might contribute to the aggregation problem. Indeed, the deletion of this region in *E. coli* L4 generates a protein that retains its capacity for regulating the S10 operon, but is more soluble than the full-length protein.<sup>2</sup>

Therefore, we constructed similar deletion derivatives of the *T. aquaticus* L4 and screened them for solubility and thermostability. A deletion between Gly<sup>45</sup> and Pro<sup>92</sup> of L4TH (corresponding to Gly<sup>42</sup>–Pro<sup>89</sup> in L4EC) rendered the protein (called L4THD7) very soluble and stable.

Before using L4THD7 for S10 mRNA binding studies we confirmed that the protein is active in inducing autogenous control in *E. coli*. First, *E. coli* cells carrying plasmids with either L4TH or L4THD7 under control of an arabinose-inducible promoter could not form colonies on plates containing arabinose, presumably because the induced *T. aquaticus* L4 proteins reduce expression of the 11 r-protein genes in the *E. coli* S10 operon, thereby blocking synthesis of ribosomes. Second, we analyzed the ability of the *T. aquaticus* L4 proteins to inhibit expression of *S10'* *lacZ* reporter genes. Induced synthesis of the full-length L4TH protein or the deletion protein (L4THD7) reduced about 3-fold the expression of an *S10'* *lacZ* gene downstream of the wild type S10 leader (Table I). This result demonstrates a substantial regulatory effect of the *T. aquaticus* L4 proteins, although the regulation is less than that of the native L4 protein. Moreover, a target plasmid containing a deletion of leader hairpin HD, which is required for *E. coli* L4-mediated transcription control, was much less responsive (Table I), suggesting that the L4TH proteins regulate transcription, and, like *E. coli* L4, require the HD hairpin. Taken together, these results show that L4THD7 is a valuable analogue of the *E. coli* L4 with respect to repression of the *E. coli* S10 operon and has the desired solubility characteristics. Highly purified protein L4THD7 was therefore used for further *in vitro* studies.

### RNA Determinants for L4 Binding

To determine a minimal binding site in the S10 leader mRNA, RNA leader fragments were assayed for binding to L4THD7 in gel shift assays (Fig. 3). S10 leader mRNA fragment D (GG62–86) does not bind to protein L4 in the gel shift experiment, and there is almost no binding to the D-loE fragment (GG64–100). The presence of helix E appears to be more important in the band shift assays than apparent from the nitrocellulose filtration experiments (*cf.* Fig. 2, *bottom*), because a little binding activity is seen with the complete helix E stem-loop structure (E, GGG86–147). Nevertheless, the minimal mRNA that shows high affinity binding is D-upE (64 nt), comprising nucleotides GG64–125 (Fig. 3, *top*). The binding of the D-upE part to L4THD7 determined by nitrocellulose filter binding is shown in Fig. 1 for comparison (*upper panel, black squares*). Binding is about 2-fold weaker than binding of L4EC to the full-length mRNA fragment.

Together with HD, the upper helix HE (nt 100–125) is strictly required for high affinity L4 interaction. The D- upE mRNA fragment, which shortcuts helix HE by connecting C100 and G132 with a UUGC-tetraloop (Fig. 1A), does not bind (*cf. D-E and D- upE* in Fig. 3, *middle*). The primary sequence requirements of the upper HE are not strict, because replacement of the upHE-loop with an U1A-loop (Fig. 1A) retains significant affinity for L4 (*D-U1AupE* in Fig. 3, *middle*).

The gel shift experiments with the L4THD7 are in good agreement with the nitrocellulose filtrations where full-length L4EC has been used, although the apparent dissociation constants are higher. However, gel shift assays are known to generate apparent  $K_D$  values up



to 1 order of magnitude higher than filter binding assays (32). Similar to the nitrocellulose competition experiments presented above, A–D and D–G bind to L4THD7 in the gel shift system (not shown). Furthermore, binding is stronger with the cognate ribosomal binding site (RNA-DI) and no binding can be detected with the dispensable A–C part of the S10 leader mRNA (Fig. 3, *bottom*). In summary, a minimal 64-nt fragment comprising HD, the ascending side of HE, and the upper HE helix is sufficient for high affinity binding of protein L4.

#### L4-S10 Leader mRNA Contacts Monitored by Iodine Footprinting

Iodine cleavage of phosphorothioated RNA is a useful tool for examining in detail RNA-protein interactions (15, 33, 34). To execute such experiments one  $\alpha$ -phosphorothioate nucleotide (A, C, G, or U) per 5'-<sup>32</sup>P-labeled transcript molecule, on average, was introduced to RNA via T7 *in vitro* transcription. The phosphorothioate S10 leader transcripts were used for two types of experiments. In an *interference experiment*, RNA-protein complexes were formed with phosphorothioate-containing RNA and isolated by binding to nitrocellulose filters. The RNA was then extracted, cleaved with iodine, and subjected to gel electrophoresis. A band that is weakened or missing on the gel indicates that the presence of a phosphorothioate moiety at the corresponding position impairs or prevents the formation of the RNA-protein complex. In a *protection experiment*, the RNA is cleaved in the complex preceding its isolation. A weakened or absent band in this experiment indicates that iodine does not have free access to the corresponding phosphorothioate in the backbone of the RNA, *i.e.* the position is protected from iodine cleavage. In this way protein interactions with the non-bridging Rp-oxygens of the RNA phosphate backbone can be mapped with atomic resolution.

Full-length S10 leader A–G and the two S10 leader fragments A–D and D–G were probed in complex with protein L4EC. Additionally, protein L4THD7 has been footprinted in complex with the minimal D-upE mRNA fragment, resulting in a pattern similar to that obtained with protein L4EC on the larger fragments.

Fig. 4A shows a section of the iodine cleavage pattern of the D–G region that contains all determinants necessary for transcription and translation control by L4. Taken together, all signals are located in helices HD and HE clearly monitoring the L4 binding site. Protein L4EC shows strong interference with 5'-phosphorothiolated U75, C76, C86, and to C94 (Fig. 4B, *stars*), and weaker interference at the positions C72, A73, G78, and A99. These same regions are also protected. Non-bridging Rp-oxygens 5' to the following nucleotides are protected against iodine cleavage in the complex with L4EC: U66, G67 (note: not shown in Fig. 4A), U69, and A74 in the 5'-strand of helix HD; in A81/85, C86-U88, A90-G95, and U97-A99 starting from HD extending to the 5' strand of lower helix HE and, finally, C111, C115, U117, U124, and G132 (not shown) in the upper helix HE (Fig. 4B, *dots*). The signals cover almost every phosphate in the backbone of the 5' part of loHE up to C100. This extensive protection could either be due to direct protein contact in this region or to structural changes induced by L4 binding to the HD region (see “Discussion”).

However, the footprint in the loop of helix HD displays very characteristic protein-RNA contacts. Interestingly, the two interference sites 5' and 3' to U75 (Fig. 4B, *red stars*) are

strongly reminiscent of the footprinting pattern of rRNA-DI in complex with L4, where O to S substitutions 5' and 3' to U321 abolish the binding of L4 (14) (Fig. 4B, inset). The three phosphates 5' to A74 and A320 and G78 and A324 are protected in the mRNA and the rRNA, respectively (Fig. 4B, red dots). Although the secondary structures are different, these data raise the intriguing possibility that helix HD of the S10 leader is a close three-dimensional mimic of the rRNA binding site (U321-loop, Fig. 4B).

### Mutational Analysis of the HD Loop

Because the footprinting data suggested direct L4 binding to the loop of hairpin HD, and because the pattern was strongly reminiscent of the interaction of L4 with its rRNA target, we analyzed the sequence requirements for L4 interaction with hairpin HD in more detail. Comparison of the *E. coli* HD loop structure with the homologous structure in S10 leader mRNAs from other  $\gamma$ -proteobacteria (7), and with the U321 loop in ribosomal RNA (L4-binding site) of different species reveals the following (Fig. 5). (i) A74 in the *E. coli* mRNA, which corresponds to position 320 in rRNA, is conserved in the S10 leader of other proteobacteria that bestow L4-mediated autogenous control; (ii) the rRNA bases 319 and 323 universally form a Watson-Crick base pair (e.g. G-C in *E. coli* and *Haloarcula marismortui*, and C-G in *T. thermophilus* and *Deinococcus radiodurans*), whereas the corresponding bases at positions 73 and 77 in the mRNA occur as noncanonical A-G or G-U combinations; and (iii) the nucleotide corresponding to C76 in *E. coli* mRNA is an adenine in 23 S rRNA throughout all three kingdoms of life (A322 in *E. coli*). Guided by these comparisons (Fig. 5) and assuming that the two L4 binding sites form similar structures, we constructed 14 mutant mRNA minimal versions and tested them for binding to protein L4THD7 in the band shift system. Selected experiments are shown in Fig. 5, together with a quantitative representation of the binding experiments in Table II.

The binding data support the idea that L4 recognizes specific primary or secondary structure features in the HD loop region. First, substitutions of the conserved A at position 74 decrease the binding affinity (Table II, mutants M1-3), particularly if the base is changed to U (Fig. 5). Second, we were interested in nucleotides 73 and 77 in the HD loop, because they are Watson-Crick paired in the 23 S rRNA target. Interestingly, the affinity for L4 for the leader was significantly reduced when bases in those positions were changed to Watson-Crick combinations (Table II, mutants M5-8), but additional changes such as C76A (M9 which resembles *E. coli* rRNA) or changes weakening the loop-closing C72-G78 base pair (M10-14) partially or fully restored binding affinity. The C76A mutation assayed by itself increased binding slightly above wild type (M4).

In summary, base exchanges in the loop of helix HD modulate the affinity of the S10 leader mRNA to L4 as much as 3-4-fold. Consistent with *in vivo* data suggesting that A74 is important, and that requirements for the HD sequence are flexible (28), none of the changes completely eliminates L4 binding. The mutational analysis reflects the phylogenetic conservation of the two RNA sites.



## DISCUSSION

### Regulatory Features of Protein L4 Are Conserved in *T. aquaticus*

The model for autogenous control of the expression of an r-protein operon assumes dual RNA binding activity of the regulating r-protein (13). That is, the protein has binding sites with affinity for both the mRNA and rRNA (1, 2, 35). Regulation of the *S10* operon transcription has been analyzed *in vivo* and in an *in vitro* transcription termination system, but proof for the presumed interaction between the S10 leader and the L4 protein has remained illusive. The high propensity of L4 for aggregation and unspecific affinity to nucleic acids have in the past thwarted attempts to demonstrate a direct interaction between L4 and leader mRNA (1, 16).

The current investigation therefore focuses on analyzing L4 interaction with the S10 leader. To circumvent the difficulties discussed above we used competition strategies and developed an L4 protein to overcome aggregation and precipitation problems. The construction of this protein, derived from *T. aquaticus* L4, took advantage of the superior stability of r-proteins from thermophiles, and the fact that the long loop covering about 50 amino acids in L4 (*cf.* Fig. 4C) (29, 30) apparently contributes to the undesirable properties of the protein, but is dispensable for regulation (17).<sup>2</sup> The resulting protein, L4THD7, with a 46-amino acid deletion in the extended loop, facilitated biochemical experiments. It also regulated the *E. coli* *S10* operon *in vivo*, apparently by the same mechanism as *E. coli* L4 (Table I).

The ability of *T. aquaticus* L4 to regulate the *E. coli* *S10* operon is interesting, because the *T. aquaticus* *S10* operon is fused with the upstream *str* operon, and hence has no S10 leader (36). One must therefore assume that L4TH does not regulate the expression of the *S10* operon in *T. aquaticus*, at least not by the mechanisms described for *E. coli*, yet the protein has maintained the determinants for that function. Similar findings have previously been made for L4 proteins from bacterial species such as *Pseudomonas aeruginosa* and *Bacillus stearothermophilus*, species that also lack an *E. coli*-like *S10* leader (7, 19). Taken together, these findings suggest that determinants necessary for the interaction of L4 with the *S10* operon mRNA of *E. coli* are conserved in other eubacteria, we presume because these same determinants are involved in ribosome assembly and/or function in the native background. This conclusion is consistent with our hypothesis that the targets of L4 in the S10 mRNA and in 23 S rRNA share structural features.

### The S10 Leader mRNA Binding Site of Protein L4

In this study we demonstrated for the first time direct and independent binding of L4 to the S10 leader RNA, using both nitrocellulose filter competition binding assays (Fig. 2) and gel shift experiments (Fig. 3). The minimal binding site for L4 binding consists of a 64-nt fragment containing hairpin HD, the 5' part of the lower HE, and the stem loop of the upper HE (Fig. 3, *top*). We propose that L4 binding to the leader requires specific interactions with the HD loop and non-sequence specific interaction with parts of HE.

The requirement for HD is supported by the following results: (i) no leader fragment lacking hairpin HD has significant binding or competition activity (Figs. 2 and 3); (ii) HD competes

by itself against binding to other, longer leader fragments and thus seems to contribute the most to the specificity of binding (Fig. 2, *bottom*); and (iii) point mutations in the loop of hairpin HD positively and negatively alter binding affinity (Fig. 5, Table II). Thus, hairpin HD is essential for binding and seems to be the main determinant for specificity. This result is consistent with *in vivo* genetic experiments showing that L4 transcription control is abolished upon deletion of hairpin HD (Table I and Ref. 11).

Nevertheless, HD does not bind by itself, so other sequences must contribute to binding. Because both A–D and D–G bind (Fig. 2), this extra energy can apparently be provided by sequences on either side of HD. The relatively weak effect of substituting the loop of HE by the U1A-loop (D-U1AupE, a change of 11 bases) implies that these sequences can add binding energy but do not contribute significantly to specificity. Deletion of the upper HE part, on the other hand, abolishes binding (D- upE, Fig. 3, *middle*). This requirement might be because of indirect effects, *e.g.* improper folding of the actual L4 target, as the upper HE is not protected by L4 binding. Consistently, other hairpins with an intact stem can substitute for the native upper HE hairpin with little or no loss of activity *in vivo* (8, 28). Nonspecific interactions have also been observed to be an essential part of specific binding and function in other RNA-protein complexes (*e.g.* Ref. 37).

### Structural Mimicry between mRNA and rRNA

The phosphorothioate footprinting results further define the hairpins HD and HE as the binding target of r-protein L4 (Fig. 4). Surprisingly, almost every phosphate in the backbone of the 5' part of loHE up to C100 is protected. We cannot differentiate whether the backbone is directly shielded from iodine cleavage by protein L4 or the footprint indicates changes in the RNA structure. We favor the latter possibility because it is difficult to see how the protein could protect one strand of the lower helix HE for more than one turn. Rather, the results suggest that in complex with L4, even in fully transcribed RNA and in the absence of an RNA polymerase complex, lower helix HE as such does not exist (*cf.* Fig. 1A versus 4B), and that its structure is influenced by L4 binding. Notably, secondary structure probing results obtained with the free RNA have been ambiguous for this particular region (6).

On the other hand, the footprint in the loop of helix HD is particularly striking because the pattern is similar to the signals that characterize the interaction of L4 with the U321-loop of 23 S rRNA (14). The rRNA binding site of L4 contains a four-helix junction (RNA-DI, Fig. 4B), which, in the ribosome (29, 30, 38), forms two longer bent helices: helices H18 and H20 stack on each other generating one continuous helix, whereas H19 stacks on the U321-loop to form the other (Fig. 4C). This way three non-consecutive RNA strands (color coded in Fig. 4, B and C) contribute bases to the helix-like arrangement that is recognized by L4: U304–G301 (*green*) and C334–G333 from H20 (*red*) base pair with G313–C318 (*blue*). Stacking on top of this helix stem, the G319–C323 pair closes the three-base U321-loop (*cyan*). Our interference results raise the interesting possibility that helix HD of the S10 leader RNA has a three-dimensional structure similar to the structure of the H19–U321-loop part of the four-helix junction: the two interference sites 5' and 3' to U75 resemble the phosphates 5' and 3' to U321 in 23 S rRNA, where O to S substitutions abolish L4 binding, and the preceding three phosphates are protected, as is the phosphate 3' to U75 and U321 in

mRNA and rRNA, respectively (Fig. 4, *red dots and stars*). The hypothesis that hairpin HD is a three-dimensional structure mimic of the rRNA-DI binding site is supported by our observation that binding of mRNA and rRNA are competitive.

The Watson-Crick 319–323 pair closing the three-base U321-loop in rRNA (Fig. 4D) is phylogenetically conserved in all three domains of life (Fig. 5), whereas the phylogenetic analysis of the mRNA suggests that the HD loop has five or more nucleotides (7). In an attempt to change the mRNA structure to a structure more like the rRNA, we changed nt A73 and/or G77 to form Watson-Crick base pairs. Most pronounced in the pyrimidine-purine combinations (*i.e.* M5 and M8), mutations predicted to form 73–77 Watson-Crick base pairs in the HD loop negatively affect the interaction with L4 (Fig. 5, Table II, M5–M8). In the crystal structures of the 50 S ribosomal subunit, the 3' nucleotide of the Watson-Crick pair (C330 of *H. marismortui* (38) and G334 of *D. radiodurans* (30)) is in a *syn*-conformation causing a turn between this and the preceding base (Fig. 4D). It appears difficult to form a Watson-Crick base pair with one base in the *syn*-conformation in the context of an A-form helix like HD, because it would similarly require a local reversal of strand direction (39).

Whereas keeping the G73–C77 Watson-Crick pair, we tried to provide a context to form a three-base loop with a similar conformation as in the rRNA by weakening and destroying the last base pair of the helix HD. Weakening of the closing base pair in the stem of HD, *i.e.* substitution of C72–G78 with A–U or U–A, indeed increased the binding affinity (M12 and M13). Replacing the C72–G78 base pair by a non-Watson-Crick combination even restores binding of the G73–C77 mutant version to wild-type levels (M10, M11). Thus, the particular backbone conformation of the three-base loop might be an important determinant for recognition of L4. One might speculate that the HD-loop does indeed only contain three nucleotides because of formation of A–G or G–U base pairs between positions 73 and 77 (Fig. 5) that could, in contrast to a Watson-Crick combination, enable a similar shape of the three-base loop.

Although a three-dimensional structure of the mRNA-L4 complex is clearly needed to substantiate these speculations, it is interesting to note that the backbone turn between A322 and C323, caused by the *syn*-conformation of the 323 base in the rRNA, is monitored in the probing results. Because of this turn, the phosphate group 5' to C323 is facing opposite to the L4 side, and is indeed the only phosphate in the loop hardly affected in the probing experiments of *both* the mRNA and rRNA L4 complexes (Fig. 4D, *green*).

### Analogies between the L4 Contacts to mRNA and rRNA Targets

Although L4 interacts with parts of Domains I, II, IV, and V in the mature 50 S subunit (30, 38), the only part of 23 S rRNA that binds to L4 in the absence of other proteins is Domain I (15). Proposing that the two RNA targets for L4 binding have a similar structure, one would expect the same part of protein L4 to interact with each of the RNA targets.

Phylogenetically conserved amino acids in the  $\alpha 4/\alpha 5$  regions of L4 (Fig. 1B) contact the RNA backbone in 23 S rRNA Domain I. In the *H. marismortui* ribosome (38) (Protein Data Bank number 1JJ1), residues Lys<sup>149</sup> (*E. coli* Lys<sup>130</sup>), Thr<sup>150</sup> (*E. coli* Thr<sup>131</sup>), and Arg<sup>205</sup> (*E.*

*coli* Arg<sup>162</sup>) bridge to the three phosphates in the A327–A329 (*E. coli* A320–A322) loop; these contacts are compatible with phosphorothioate footprinting experiments (Fig. 4D) (14, 15). The only base directly recognized in the *H. marismortui* rRNA-Domain I L4 binding site is A327 (*E. coli* A320), which is contacted by the universally conserved asparagine 206 (*E. coli* Arg<sup>163</sup>) and glutamine 151 (*E. coli* Lys<sup>132</sup>). Mutations of the corresponding adenine in the HD loop of the mRNA decrease binding affinity (Table II, M1–M3) and affect regulation *in vivo* (28).

Mutations in the  $\alpha 4/\alpha 5$  region of *E. coli* L4 (Thr<sup>131</sup>, Leu<sup>134</sup>, Ala<sup>160</sup>, and Val<sup>167</sup>) abolish L4-dependent regulation *in vivo* (17). Furthermore, modifications in the  $\alpha 4/\alpha 5$  region of L4 from *T. maritima* bestow on this protein a capacity to regulate the *E. coli* S10 operon not possessed by wild-type *T. maritima* L4 protein (40). Thus, amino acids in L4 that contact 23 S rRNA Domain I or are close to these L4 residues may also be involved in recognizing the HD mRNA region, supporting the analogy between the two binding events.

### Conclusions on the Mechanism of L4-mediated Transcription Termination

Studies of Rho-independent transcription termination suggest that cessation or prolongation of transcription is caused by changes in the conformation of the nascent RNA chain (41, 42). These changes could be effected by protein factors, such as NusA and  $\lambda$ N protein (43, 44), or ribosomal proteins (45). Analysis of transcription complexes paused at other terminators (46, 47) suggests that exactly the minimal D-upE segment would be accessible to L4 binding in the paused complex. L4-induced termination of transcription at the S10 attenuator requires both L4 and NusA (12, 48, 49). In the current study we have found that L4 can bind to the S10 leader mRNA in the absence of NusA. The effect of NusA is thus not related to L4 binding. Our footprint data suggest changes in the RNA leader structure induced by L4 binding. If so, NusA might be required for propagation of this signal to the RNA polymerase during the transcription termination event.

### Acknowledgments

We thank Beatriz Cebolla for help with initial experiments, Alexander Serganov for the pAB5313 S15-mRNA plasmid, and Alexander Mankin for the L4 *T. aquaticus* clone.

### References

1. Zengel JM, Lindahl L. Prog Nucleic Acids Res Mol Biol. 1994; 47:331–370.
2. Keener, J.; Nomura, M. Escherichia coli and Salmonella typhimurium. Neidhardt, FC., editor. American Society for Microbiology; Washington, D. C: 1996. p. 1417-1431.
3. Zengel JM, Mueckl D, Lindahl L. Cell. 1980; 21:523–535. [PubMed: 6157482]
4. Yates JL, Nomura M. Cell. 1980; 21:517–522. [PubMed: 6996835]
5. Lindahl L, Archer R, Zengel JM. Cell. 1983; 33:241–248. [PubMed: 6380754]
6. Shen P, Zengel JM, Lindahl L. Nucleic Acids Res. 1988; 16:8905–8924. [PubMed: 3050893]
7. Allen T, Shen P, Samsel L, Liu R, Lindahl L, Zengel JM. J Bacteriol. 1999; 181:6124–6132. [PubMed: 10498727]
8. Freedman LP, Zengel JM, Archer RH, Lindahl L. Proc Natl Acad Sci U S A. 1987; 84:6516–6520. [PubMed: 2442760]
9. Zengel JM, Lindahl L. J Mol Biol. 1990; 213:67–78. [PubMed: 1692593]
10. Sha Y, Lindahl L, Zengel JM. J Mol Biol. 1995; 245:486–498. [PubMed: 7531246]

11. Zengel JM, Lindahl L. *J Bacteriol.* 1996; 178:2383–2387. [PubMed: 8636042]
12. Sha Y, Lindahl L, Zengel JM. *J Mol Biol.* 1995; 245:474–485. [PubMed: 7844821]
13. Nomura M, Yates JL, Dean D, Post LE. *Proc Natl Acad Sci U S A.* 1980; 77:7084–7088. [PubMed: 7012833]
14. Stelzl U, Spahn CMT, Nierhaus KH. *Proc Natl Acad Sci U S A.* 2000; 97:4597–4602. [PubMed: 10781065]
15. Stelzl U, Nierhaus KH. *RNA.* 2001; 7:598–609. [PubMed: 11345438]
16. Zengel JM, Lindahl L. *Nucleic Acids Res.* 1993; 21:2429–2435. [PubMed: 7685080]
17. Li X, Lindahl L, Zengel JM. *RNA.* 1996; 2:24–37. [PubMed: 8846294]
18. Diedrich G, Burkhardt N, Nierhaus KH. *Protein Expr Purif.* 1997; 10:42–50. [PubMed: 9179289]
19. Li X, Lindahl L, Sha Y, Zengel JM. *J Bacteriol.* 1997; 179:7046–7054. [PubMed: 9371452]
20. Stelzl U, Spahn CMT, Nierhaus KH. *Methods Enzymol.* 2000; 318:251–268. [PubMed: 10889993]
21. Lin SY, Riggs AD. *J Mol Biol.* 1972; 72:671–690. [PubMed: 4573844]
22. Schlax PJ, Xavier KA, Gluick TC, Draper DE. *J Biol Chem.* 2001; 276:38494–38501. [PubMed: 11504736]
23. Robert F, Brakier-Gingras L. *Nucleic Acids Res.* 2001; 29:677–682. [PubMed: 11160889]
24. Osswald M, Greuer B, Brimacombe R. *Nucleic Acids Res.* 1990; 18:6755–6760. [PubMed: 1702198]
25. Serganov AA, Masquida B, Westhof E, Cachia C, Portier C, Garber M, Ehresmann B, Ehresmann C. *RNA.* 1996; 2:1124–1138. [PubMed: 8903343]
26. Gerstner RB, Pak Y, Draper DE. *Biochemistry.* 2001; 40:7165–7173. [PubMed: 11401563]
27. Philippe C, Portier C, Mougél M, Grunberg-Manago M, Ebel JP, Ehresmann B, Ehresmann C. *J Mol Biol.* 1990; 211:415–426. [PubMed: 2407855]
28. Zengel JM, Sha Y, Lindahl L. *RNA.* 2002; 8:572–578. [PubMed: 12022224]
29. Ban N, Nissen P, Hansen J, Moore PB, Steitz TA. *Science.* 2000; 289:905–920. [PubMed: 10937989]
30. Harms J, Schluenzen F, Zarivach R, Bashan A, Gat S, Agmon I, Bartels H, Franceschi F, Yonath A. *Cell.* 2001; 107:679–688. [PubMed: 11733066]
31. Worbs M, Huber R, Wahl MC. *EMBO J.* 2000; 19:807–818. [PubMed: 10698923]
32. Draper DE, Deckman IC, Vartikar JV. *Methods Enzymol.* 1988; 164:203–220. [PubMed: 3071663]
33. Verma S, Eckstein F. *Annu Rev Biochem.* 1998; 67:99–134. [PubMed: 9759484]
34. Strobel SA. *Curr Opin Struct Biol.* 1999; 9:346–352. [PubMed: 10361087]
35. Draper D. *Trends Biochem Sci.* 1989; 14:335–338. [PubMed: 2678632]
36. Pfeiffer T, Jorcke D, Feltens R, Hartmann RK. *Gene (Amst).* 1995; 167:141–145. [PubMed: 8566766]
37. Torres-Larios A, Dock-Bregeon AC, Romby P, Rees B, Sankaranarayanan R, Caillet J, Springer M, Ehresmann C, Ehresmann B, Moras D. *Nat Struct Biol.* 2002; 9:343–347. [PubMed: 11953757]
38. Klein DJ, Schmeing TM, Moore PB, Steitz TA. *EMBO J.* 2001; 20:4214–4221. [PubMed: 11483524]
39. Leontis NB, Westhof E. *RNA.* 2001; 7:499–512. [PubMed: 11345429]
40. Worbs M, Wahl MC, Lindahl L, Zengel JM. *Biochimie (Paris).* 2002; 84:731–743.
41. Henkin TM. *Curr Opin Microbiol.* 2000; 3:149–153. [PubMed: 10745002]
42. Landick R. *Cell.* 2001; 105:567–570. [PubMed: 11389826]
43. Gusarov I, Nudler E. *Cell.* 2001; 107:437–449. [PubMed: 11719185]
44. Touloukhonov I, Artsimovitch I, Landrick R. *Science.* 2001; 292:730–733. [PubMed: 11326100]
45. Torres M, Condon C, Balada JM, Squires C, Squires CL. *EMBO J.* 2001; 20:3811–3820. [PubMed: 11447122]
46. Artsimovitch I, Landick R. *Genes Dev.* 1998; 12:3110–3122. [PubMed: 9765211]

47. Korzheva N, Mustaev A, Kozlov M, Malhotra A, Nikiforov V, Goldfab A, Darst SA. *Science*. 2000; 289:619–625. [PubMed: 10915625]
48. Zengel JM, Lindahl L. *Proc Natl Acad Sci U S A*. 1990; 87:2675–2679. [PubMed: 2157208]
49. Zengel JM, Lindahl L. *Genes Dev*. 1992; 6:2655–2662. [PubMed: 1285127]

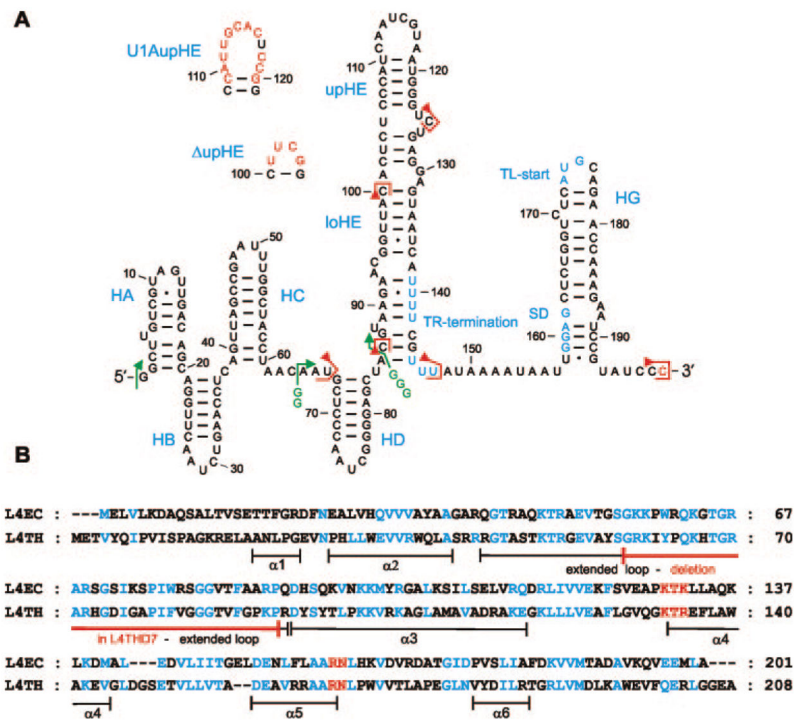
Author Manuscript

Author Manuscript

Author Manuscript

Author Manuscript



**Fig. 1.**

A, secondary structure of the *E. coli* S10 leader mRNA (6, 7) and constructs derived from it. *Green arrows*, with the additional Gs for efficient T7 RNA polymerase run-off transcription, indicate transcription start sites. *Red brackets* indicate the ends of the RNA constructs. Deviations from the wild-type *E. coli* sequence are indicated by *red* nucleotides. The six helical structures (HA, HB, HC, HD, loHE (lower part of HE), upHE (upper part of HE), and HG), the Rho-independent transcription termination site (*TR-termination*), the Shine-Dalgarno sequence (*SD*), the translation initiation codon (*TL-start*), and the helix nomenclature are shown in *blue*. B, sequence alignment of *E. coli* L4 and L4 from *T. aquaticus*. Conserved amino acids are indicated in *blue*, residues putatively involved in RNA binding are shown in *red* (see text). The 46-amino acid deletion of protein L4THD7 within the extended loop is indicated in *red* (cf. Fig. 4C).

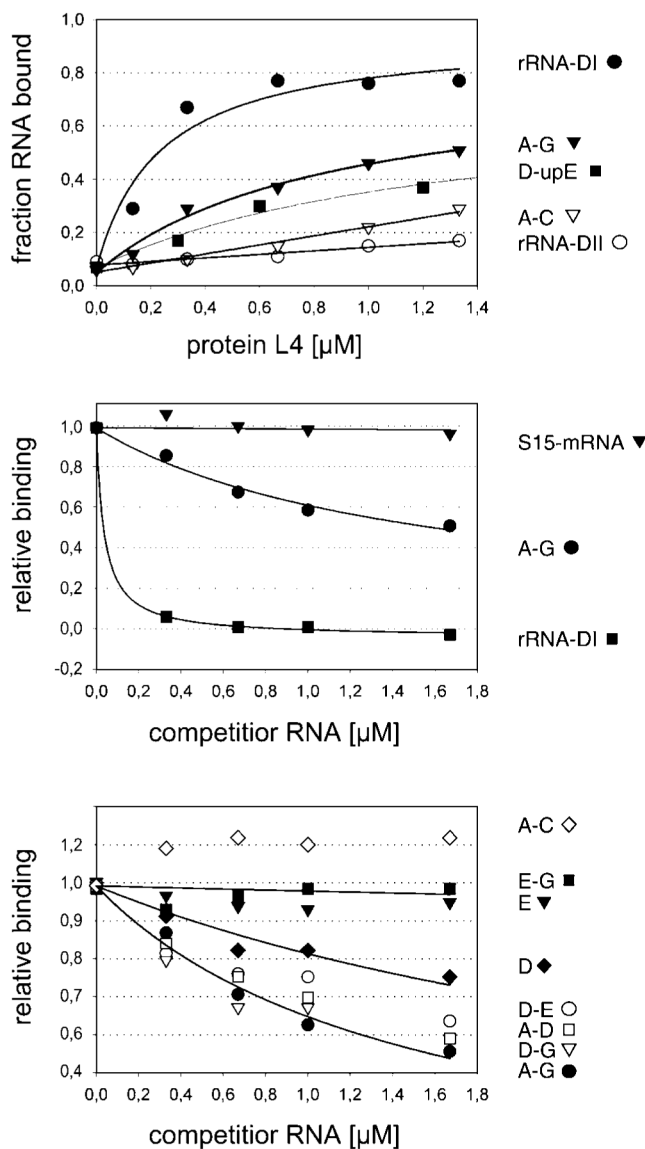


**Fig. 2. Nitrocellulose filter binding assays**

*Symbols indicate different RNA fragments. Top*, binding of the S10 leader mRNA and rRNA fragments to L4EC, except for *filled squares* that show binding of protein L4THD7 to the D-upE minimal mRNA fragment (0.067  $\mu\text{M}$  [ $^{32}\text{P}$ ]RNAs, 20 mM Hepes-KOH (pH 7.4), 250 mM  $\text{NH}_4\text{Cl}$ , 4 mM  $\text{MgCl}_2$ , 0.01 mg/ml BSA, 1  $\mu\text{M}$  tRNA). Binding curves are best fits to the data resulting an apparent  $K_D = 0.23 \mu\text{M}$  for L4EC bound to rRNA-DI (*filled circles*), an apparent  $K_D = 0.80 \mu\text{M}$  for L4EC bound to the full-length mRNA (A-G, *filled triangles*), and an apparent  $K_D = 1.3 \mu\text{M}$  for the L4THD7-D-upE interaction (*filled squares, thin line*). We note that when bound to mRNA fragments the retention efficiency for L4THD7 (0.60) is lower than for L4EC (0.76), which makes a direct comparison of the two curves difficult. *Middle*, competition of L4 binding to full-length leader A-G by unrelated RNAs (0.33  $\mu\text{M}$  [ $^{32}\text{P}$ ]RNA A-G, 0.67  $\mu\text{M}$  protein L4EC, 20 mM Hepes-KOH (pH 7.4), 225 mM  $\text{NH}_4\text{Cl}$ , 4 mM  $\text{MgCl}_2$ , 0.01 mg/ml BSA). *Bottom*, competition of L4 binding to full-length leader A-G

by S10 leader mRNA fragments (conditions like in *middle panel*). A–C, nt 1–66; E, nt GGG86–147; E–G, nt GGG86–197C; D, nt GG62–86; D–E, GG62–147; A–D, 1–86; D–G, GG62–197C; and A–G, 1–197C (*cf.* Fig. 1). The competition curves were calculated as described under “Experimental Procedures.” The best fit gave a  $K_D$  of 0.82  $\mu\text{M}$  for the competition with the A–G mRNA (*filled circle, middle and bottom*), a  $K_D$  of 1.87  $\mu\text{M}$  for the helix D fragment (*filled diamond*), and a  $K_D$  of 30.7  $\mu\text{M}$  for the E–G mRNA fragment (*filled squares*).

Author Manuscript

Author Manuscript

Author Manuscript

Author Manuscript

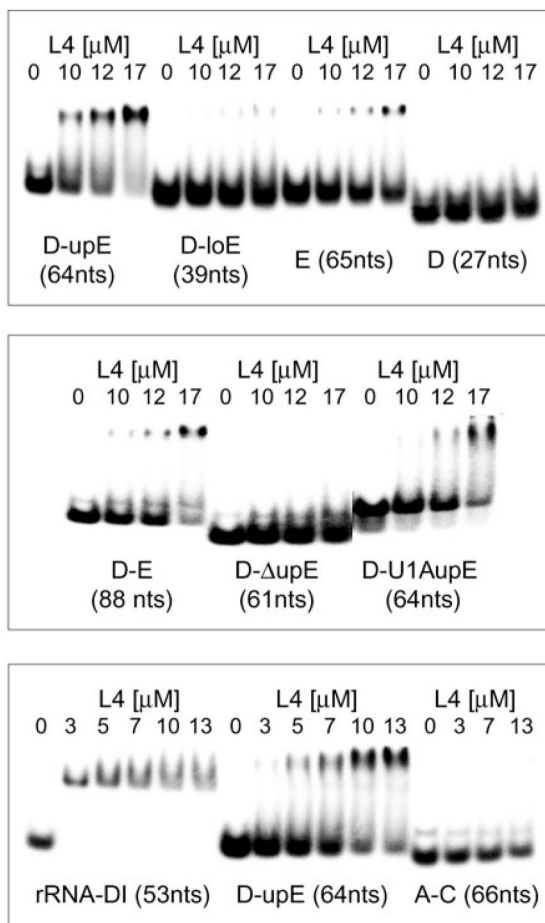


**Fig. 3. Gel shift assays**

5% polyacrylamid native gels (20 mM HEPES-KOH (pH 7.4), 100 mM  $\text{NH}_4\text{Cl}$ , 4 mM  $\text{MgCl}_2$ , 0.01 mg/ml AcBSA) with 5  $\mu\text{M}$  [ $^{32}\text{P}$ ]RNAs and L4THD7 as indicated, are shown. *Top*, the minimal fragment for high affinity binding is D-upE (GG64–125), whereas D-loE (GG64–100), E (GGG86–147), and D (GG62–86) show no or little binding. *Middle*, upper HE is necessary for binding (D-E (GG62–147) *versus* D-upE (GG62–100-UUCG-132–147)) but there are little primary sequence requirements (D-U1AupE (GG64–108-CAUUGCACUCCG-121–125)). *Bottom*, binding of the minimal D-upE fragment is compared with the interaction with rRNA-DI (23 S ribosomal RNA fragment GG295–343CC) and the A-C (1–66) part of the S10 leader that has approximately the same size, but is dispensable for function *in vivo*. Note that the different lengths of the internally  $^{32}\text{P}$ -labeled RNAs result in different specific activities. Also, for better comparison, two similar gel shift experiments with the minimal D-upE fragment are displayed, one in the *top* and the other in the *bottom panel*.

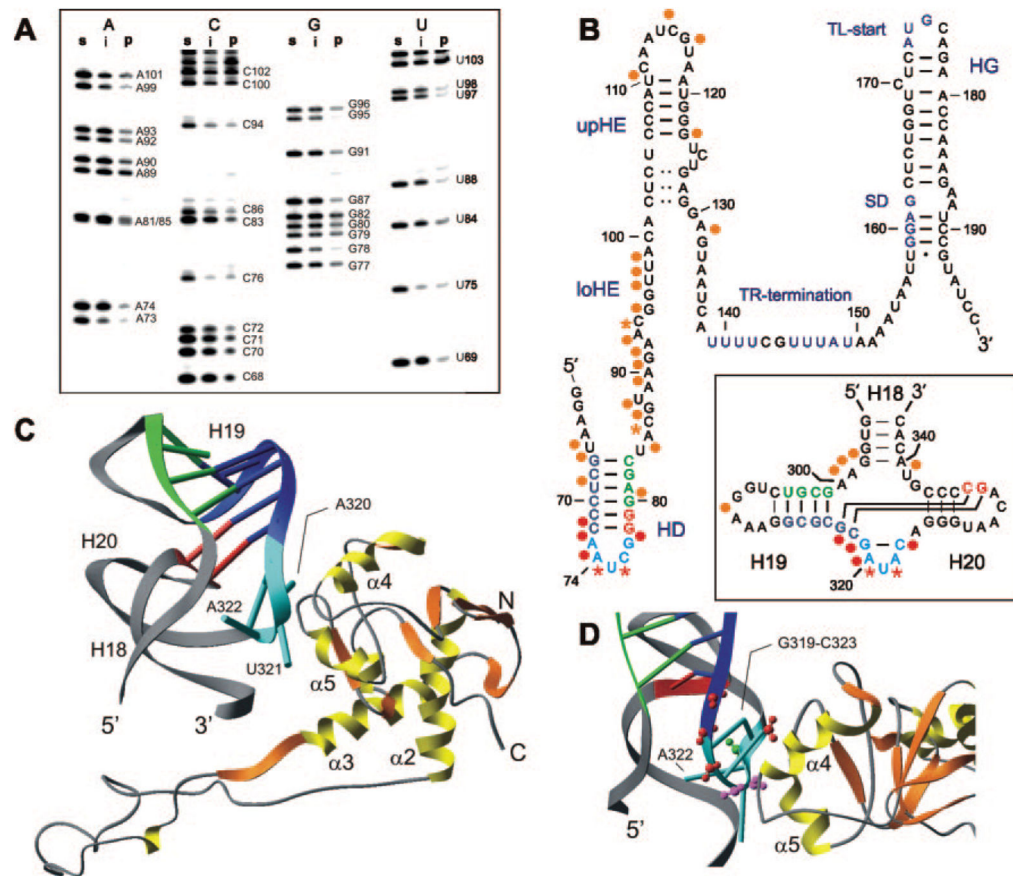


**Fig. 4. Iodine footprinting of the S10 leader mRNA in complex with protein L4**

**A**, probing of mRNA fragment D–G in complex with L4EC (section of a 10% denaturing polyacrylamide/urea gel). *s*, solution lane; *i*, interference lane; *p*, protection lane. We note that, for all constructs probed, the G80 to G87 region is strongly compressed. In particular, A81 and A85 are hardly separated and the bands representing C83 and U84 migrate faster than expected. The primary sequence of the constructs has unambiguously been determined on the DNA level by sequencing. Such behavior is because of the structure of the RNA and independent of the interaction with L4, because after iodine cleavage of mRNA fragments in the absence of L4 (*lane s*) the bands migrate to the same positions. **B**, secondary structure of the D–G S10 leader RNA fragment (*cf.* Fig. 1) indicating probing results: *stars* for interference and *full circles* for protections. For comparison, the *inset* shows the interference and protection patterns of the rRNA-DI 23 S fragment in complex with protein L4 (14). Nucleotides in *green* (301–304), *blue* (313–323), and *red* (333–334) form a helix-like structure shown in **C** using the same color code. Protection and interference signals in *red* are to emphasize similarities between the two RNAs. **C**, from the 3.1-Å crystal structure of the 50 S subunit of *D. radiodurans* 50 S subunit (Protein Data Bank number 1KC9 (30)) with *E. coli* numbering: the RNA-DI binding site (*D. radiodurans* nt 312–315, *green*; 344–345, *red*; 324–329, *blue*; and 330–334 in *cyan*) and protein L4 ( $\alpha$ -helices in *yellow*,  $\beta$ -sheets in *orange*, nomenclature follows (31)). **D**, close up of the rRNA-L4 interaction site displaying the phosphorothioate footprinting results. Protected phosphates in *red*, sites of

interference in *magenta*. The *green* phosphate, facing away from L4, is not affected by L4 binding in the probing experiments.

Author Manuscript

Author Manuscript

Author Manuscript

Author Manuscript



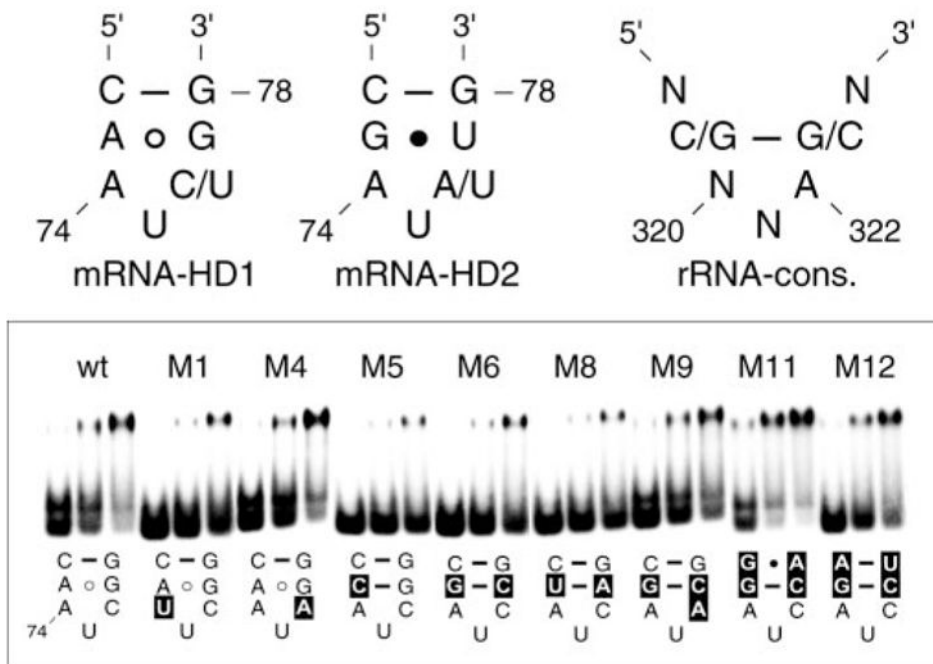


**Fig. 5. Phylogenetic comparison of the HD-loop in S10 mRNA leader sequences and the rRNA U321-loop of Domain I of 23 S RNA**  
 mRNA-HD1 is found in *E. coli* (C76), *Salmonella typhimurium* (C76), and *Citrobacter freundii* (U76). mRNA-HD2 occurs in *Yersinia enterocolitica* (A76), *Serratia marcescens* (A76), *Morganella morganii* (A76), and *Haemophilus influenzae* (U76). All these leader sequences have shown an L4-dependent regulatory response *in vivo* (7). *rRNA-cons.* indicates the minimal consensus sequence from all three kingdoms of life. The 319–323 Watson-Crick base pair and A322 are universally conserved. *Boxed*, gel shift assays (5% polyacrylamide gel, 20 mM Hepes-KOH (pH 7.4), 100 mM NH<sub>4</sub>Cl, 4 mM MgCl<sub>2</sub>, 0.01 mg/ml AcBSA). For every RNA mutant (3 lanes each), protein L4THD7 was added to 7.5, 12, and 17 μM. [<sup>32</sup>P]RNA mutants (5 μM) are D-upE minimal fragments. Mutated nucleotides are indicated on the *black background* in the HD-loop secondary structures (see also Table II).

**Table I**  
**In vivo analysis of autogenous regulation by *T. aquaticus* L4 in *E. coli***

Cells containing the indicated target plasmid and a plasmid with the indicated L4 gene were induced with isopropyl-1-thio- $\beta$ -D-galactopyranoside or with isopropyl-1-thio- $\beta$ -D-galactopyranoside and arabinose and then pulse-labeled (in duplicate) with [ $^{35}$ S]methionine before and after the induction of L4. Total cell extracts were fractionated on a 7.5% SDS-PAGE gel and analyzed using a PhosphorImager. The ratio of *S10'*'  $\beta$ -gal synthesis rates in the presence and absence of arabinose for each protein was determined from a minimum of two independent experiments. The average is shown, with the standard deviation given in parentheses.

L4 protein	L4 regulation of <i>S10L-S10'</i> ' <i>lacZ</i>	L4 regulation of <i>S10L HD-S10'</i> ' <i>lacZ</i>
L4EC	0.09 ( $\pm$ 0.02)	0.54 ( $\pm$ 0.02)
L4TH	0.31 ( $\pm$ 0.03)	0.71 ( $\pm$ 0.06)
L4THD7	0.41 ( $\pm$ 0.07)	0.81 ( $\pm$ 0.06)

Author Manuscript

Author Manuscript

Author Manuscript

Author Manuscript

**Table II**  
**Quantitative analysis of the effect of mutations in the loop of helix HD on the interaction with L4THD7**

Binding, calculated as fraction of RNA in the complex, was normalized to wild-type binding. Because binding is not in saturation, but rather shows a pseudo-linear behavior at low protein concentrations, normalized values of the three different protein concentrations were combined. Experiments as displayed in Fig. 5 have been done for each mutant at least three times.

Name/position	72	73	74	75	76	77	78	Binding	±
D-upE-wt	C	A	A	U	C	G	G	1.00	
M1			U					0.48	0.10
M2			C					0.66	0.15
M3			G					0.76	0.19
M4				A				1.12	0.15
M5		C						0.31	0.07
M6		G			C			0.49	0.18
M7					U			0.56	0.13
M8		U			A			0.28	0.09
M9		G		A	C			0.84	0.10
M10	A	G			C			0.95	0.09
M11	G	G			C	A		1.07	0.06
M12	A	G			C	U		0.68	0.19
M13	U	G			C	A		0.63	0.17
M14	U	G		A	C	A		0.68	0.22